JOC*Article*

An Experimental and Computational Analysis on the Differential Role of the Positional Isomers of Symmetric Bis-2-(pyridyl)-1*H*-benzimidazoles as DNA Binding Agents

Padmaparna Chaudhuri,[†] Bishwajit Ganguly,*[,‡] and Santanu Bhattacharya*[,†,§]

Department of Organic Chemistry, Indian Institute of Science, Bangalore 560 012, India, Central Salt and Marine Chemicals Research Institute, Bhavnagar, Gujarat 364 002, India, and Chemical Biology Unit, Jawaharlal Nehru Centre of Advanced Scientific Research, Bangalore 560 012, India

sb@orgchem.iisc.ernet.in

Received September 20, 2006

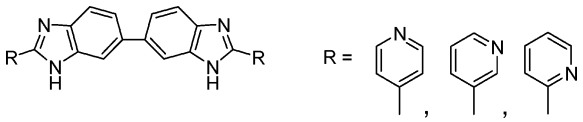

Three symmetrical positional isomers of bis-2-(*n*-pyridyl)-1*H*-benzimidazoles ($n = 2, 3, 4$) were synthesized and DNA binding studies were performed with these isomeric derivatives. Like bisbenzimidazole compound Hoechst 33258, these molecules also demonstrate AT-specific DNA binding. The binding affinities of 3-pyridine (*m*-pyben) and 4-pyridine (*p*-pyben) derivatized bisbenzimidazoles to double-stranded DNA were significantly higher compared to 2-pyridine derivatized benzimidazole *o*-pyben. This has been established by combined experimental results of isothermal fluorescence titration, circular dichroism, and thermal denaturation of DNA. To rationalize the origin of their differential binding characteristics with double-stranded DNA, computational structural analyses of the uncomplexed ligands were performed using ab initio/Density Functional Theory. The molecular conformations of the symmetric head-to-head bisbenzimidazoles have been computed. The existence of intramolecular hydrogen bonding was established in *o*-pyben, which confers a conformational rigidity to the molecule about the bond connecting the pyridine and benzimidazole units. This might cause reduction in its binding affinity to double-stranded DNA compared to its *para* and *meta* counterparts. Additionally, the predicted stable conformations for *p*-, *m*-, and *o*-pyben at the B3LYP/6-31G* and RHF/6-31G* levels were further supported by experimental pK_a determination. The results provide important information on the molecular recognition process of such symmetric head to head bisbenzimidazoles toward duplex DNA.

Introduction

Drugs capable of targeting specific sequences in *B*-DNA are of considerable interest because of their potential use in anticancer chemotherapy.[1−3] Among them, natural minor groove binding drugs, e.g., netropsin or distamycin[4] and their analogues[5,6] and synthetic bisbenzimidazole derivatives[7] such as Hoechst 33258, have been extensively studied in relation to their interaction with the DNA double helix.

Hoechst 33258 (Hoechst) consists essentially of a bisbenzimidazolic core unit appended to *N*-methyl piperazine and phenol groups at either end (Chart 1). Hoechst, which is a chromosome-staining agent with antihelmintic activity, binds strongly to the minor groove of double-stranded (*ds*-) DNA with specificity for AT-rich sequences.[7] The interaction of Hoechst with DNA has been extensively studied using X-ray crystallography[8,9] and NMR spectroscopy.[10,11] The molecule is endowed with the essential attributes of a typical minor groove

* To whom correspondence should be addressed. Phone: +(91)-80-2293-2664. Fax: +(91)-80-23600529.
[†] Indian Institute of Science.
[‡] Central Salt and Marine Chemicals Research Institute.
[§] Jawaharlal Nehru Centre of Advanced Scientific Research.

(1) Yang, X. L.; Wang, A. H. *J. Pharmacol. Ther.* **1999**, *83*, 181.
(2) Hurley, L. H. *Nat. Rev. Cancer* **2002**, *2*, 188.
(3) Martinez, R.; Chacon-Garcia, L. *Curr. Med. Chem.* **2005**, *12*, 127.
(4) Bailly, C.; Chaires, J. B. *Bioconjugate Chem.* **1998**, *9*, 513.
(5) Bhattacharya, S.; Thomas, M. C*hem. Commun*. **2001**, 1464.
(6) Dervan, P. B. *Bioorg. Med. Chem.* **2001**, *9*, 2215.
(7) Lootiens, F. G.; Regenfuss, P.; Zechel, A.; Dumortier, L.; Clegg, R. M. *Biochemistry* **1990**, *29*, 9029.
(8) Pjura, P. E.; Grzeskoviak, K.; Dickerson, R. E. *J. Mol. Biol.* **1987**, *197*, 257.
(9) Quintana, J. R.; Lipanov, A. A.; Dickerson, R. E. *Biochemistry* **1991**, *30*, 10294.
(10) Embrey, K. J.; Searle, M. S.; Craik, D. J. *Eur. J. Biochem.* **1993**, *211*, 437.
(11) Fede, A.; Billeter, M.; Leupin, W.; Wuthrich, K. *Structure* **1993**, *1*, 177.

10.1021/jo0619433 CCC: $37.00
Published on Web 02/17/2007

CHART 1. Structures of Hoechst 33258 and the Three Pyridine Derivatized Symmetrical Bisbenzimidazoles

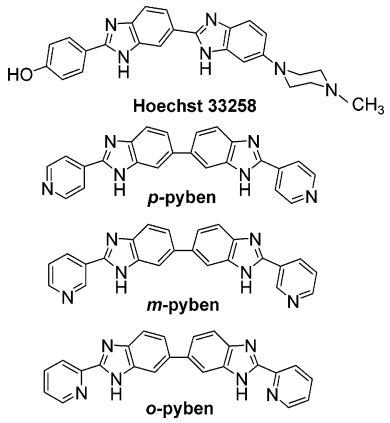

binding ligand, namely, an overall crescent shape to match the helical pitch of the DNA minor groove and suitable hydrogen-bond donors capable of hydrogen bonding with the nucleobases. The cationic charge in Hoechst further facilitates its favorable electrostatic interaction with the polyanionic phosphodiester backbone of DNA.[12] Additionally, the molecule has sufficient conformational flexibility about the bonds connecting the individual units that enables it to adopt optimum shape complimentarity with the minor groove in order to maximize van der Waals attraction.[12]

As a result, Hoechst has emerged as a model for synthetic ligand design. Several benzimidazole derivatives have been synthesized with the aim to increase the *ds*-DNA binding affinity and specificity.[13−15] Chemical modifications at the phenolic group[16] and also in the nature of the cationic charge have been performed,[17] but despite its numerous applications, multistep syntheses of Hoechst and its derivatives are often quite cumbersome, involving difficult purification steps.[14,18]

To alleviate some of these difficulties, a new class of simple symmetrical bisbenzimidazole-based DNA minor groove binding agents were developed by Neidle and co-workers.[19] The DNA binding property of these molecules and their activities as antitumor agents have also been evaluated.[19,20] Our aim in this work has been to develop an even simpler set of symmetrical bisbenzimidazoles, which would involve just one-step synthesis and at the same time ensure that the resulting molecules retain the essential attributes of a DNA groove binding molecule, namely, an overall crescent shape and hydrogen bond forming groups. Toward this end we prepared three isomeric bis-2-(*n*-pyridyl)-1*H*-benzimidazole derivatives (Chart 1) in one step, upon oxidative condensation of either 2-, 3-, or 4-pyridine carboxaldehydes with 3,3′-diaminobenzidine.

DNA binding studies showed a dramatic difference in the binding of the *o*-pyridine derivative (*o*-pyben) compared to its *meta* and *para* analogues, denoted by *m*-pyben and *p*-pyben, respectively. Whereas *p*-pyben and *m*-pyben showed high affinity binding to *ds*-DNA as seen from the greater thermal stability of duplex DNA on ligand binding and fluorescence and circular dichroism studies, the binding of *o*-pyben was significantly weak. We sought to answer this differential DNA binding behavior of the isomeric compounds by examining their intrinsic structural features.

Accordingly, to examine the difference in binding of the bisbenzimidazole derivatives to *ds*-DNA, calculations using Density Functional Theory (DFT) were performed. Computational studies on minor groove binding agents employing quantum chemical methods are rather limited. In principle, quantum chemical methods provide more reliable predictions of molecular properties than methods based on empirical force fields and have been used by Aleman and co-workers for determining conformational preference and acid−base properties of parent Hoechst 33258.[21−24] Therefore, we have investigated at DFT level the conformational preferences of the bisbenzimidazole derivatives to explain the differences in their binding affinity toward the minor groove of *ds*-DNA. The conformations of bisbenzimidazole derivatives have been examined initially in the gas phase. Furthermore, a self-consistent reaction field (SCRF) procedure has been employed to account for the influence of hydration in the aqueous media. The calculated structures of bisbenzimidazoles have been compared with the X-ray determined crystal structure (PDB code 1FTD) of a related symmetrical bisbenzimidazole derivative.[20] These results provide important information on the molecular recognition and binding process of uncomplexed bisbenzimidazoles toward the double-stranded DNA. Additionally, we also determined the pK_a values of these ligands experimentally in water to shed light on the geometry of the molecules that distinguishes the *ortho* derivative from the *meta* and *para* analogues in its DNA binding affinity.

Results and Discussion

Ligands. The similarity of these molecules to parent Hoechst 33258 lies in the nature of the bisbenzimidazole core unit. On the other hand, the features that distinguish them from Hoechst are many. Unlike Hoechst, they are symmetrical, with the benzimidazoles linked by phenyl−phenyl bonds. Also, instead of one piperazine unit (a sp^3 hybridized secondary amine) in Hoechst 33258, these molecules bear aromatic pyridine moieties (sp^2 hybridized N) at both the termini. The pK_a of the terminal piperazine N in Hoechst being ∼7.8,[25] the molecule is positively charged at physiological pH. In contrast pyridine N has a pK_a of ∼5.2,[26] and thus the neutral species of these pyridine derivatized molecules are expected to be most predominant at physiological pH. The differences in pK_a, hybridization state, and number (two vs one) of the terminal amines make the molecules distinct from Hoechst. Moreover, the DNA base pair

(12) Wood, A. A.; Nunn, C. M.; Czarny, A.; Boykin, D. W.; Neidle, S. *Nucleic Acid Res.* **1995**, *23*, 3678.
(13) Satz, A. L.; Bruice, T. C. *J. Am. Chem. Soc.* **2001**, *123*, 2469.
(14) Behrens, C.; Harrit, N.; Nielsen, P. E. *Bioconjugate Chem.* **2001**, *12*, 1021.
(15) Tanada, M.; Tsujita, S.; Sasaki, S. *J. Org. Chem.* **2006**, *71*, 125.
(16) Clark, G. R.; Squire, C. J.; Gray, E. J.; Leupin, W.; Neidle, S. *Nucleic Acid Res.* **1996**, *24*, 4882.
(17) Bostock-Smith, C. E.; Searle, M. S. *Nucleic Acid Res.* **1999**, *27*, 1619.
(18) Minehan, T. G.; Gottwald, K.; Dervan, P. B. *Helv. Chim. Acta* **2000**, *83*, 2197.
(19) Neidle, S.; Mann, J.; Rayner, E. L.; Baron, A.; Boahen, Y. O.; Simpson, I. J.; Smith, N. J.; Fox, K. R.; Hartley, J. A.; Kelland, L. R. *Chem. Commun.* **1999**, 929.
(20) Mann, J; Baron, A.; Opoku-Boahen, Y.; Johansson, E.; Parkinson, G.; Kelland, L. R.; Neidle, S. *J. Med. Chem.* **2001**, *44*, 138.
(21) Vega, M. C.; Coll, M.; Alemán, C. *Eur. J. Biochem.* **1996**, 376.
(22) Alemán, C. *Theor. Chem. Acc.* **1998**, *99*, 312.
(23) Alemán, C.; Adhikary, A.; Zanuy, D., and Casanovas, J. *J. Biomol. Struct. Dyn.* **2002**, *20*, 301.
(24) Aleman, C.; Namba, A. M.; Casanovas, J. *J. Biomol. Struct. Dyn.* **2005**, *23*, 29.
(25) Ladinig, M.; Leupin, W.; Meuwly, M.; Respondek, M.; Wirz, J.; Zoete, V. *Helv. Chim. Acta* **2005**, *88*, 53.
(26) Krygowski, T. M.; Szatyowicz, H.; Zachara, J. E. *J. Org. Chem.* **2005**, *70*, 8859.

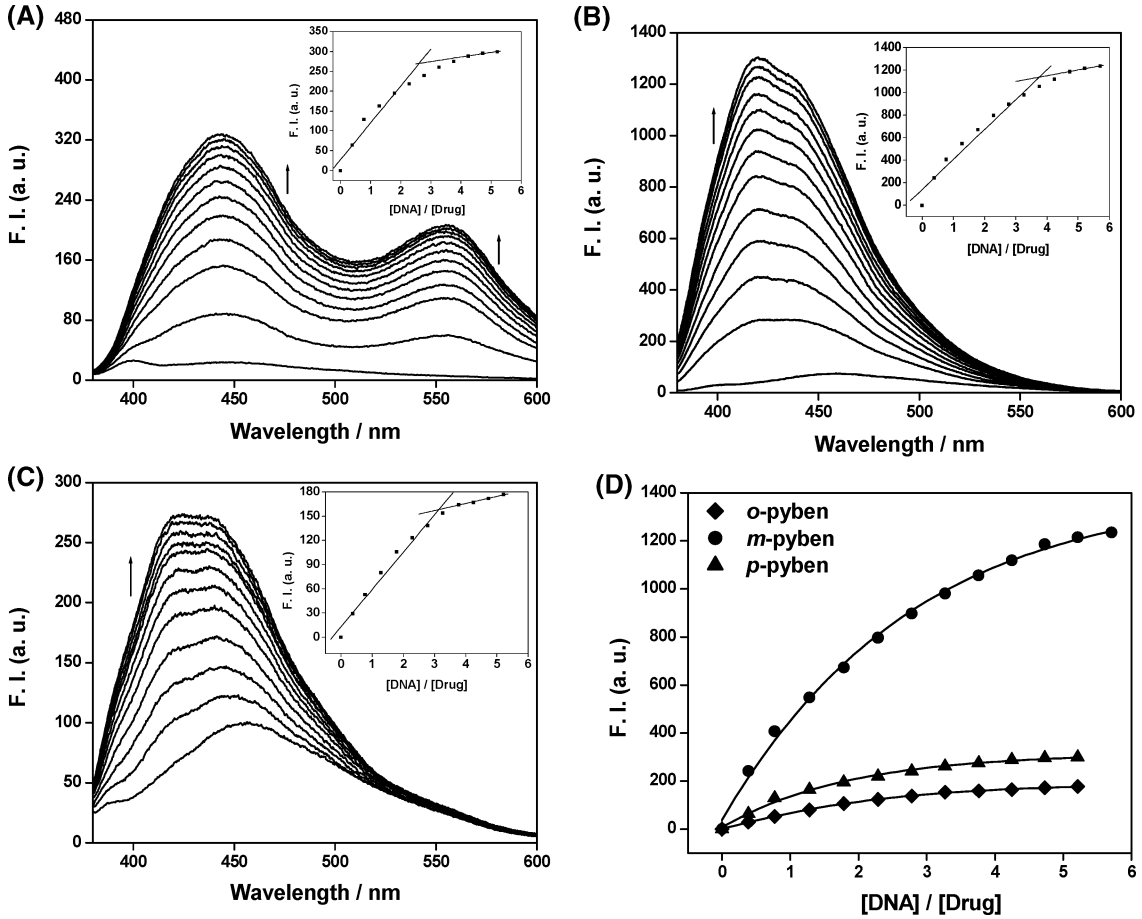

FIGURE 1. Fluorescence enhancement on addition of [Poly(dA)-Poly(dT)] into a 2 μM solution of (A) *p*-pyben, (B) *m*-pyben, and (C) *o*-pyben in 50 mM Tris-HCl, 100 mM NaCl, and 0.1 mM EDTA buffer, indicated by the upward arrows. The insets show fluorescence intensity at emission maxima versus [DNA]/[drug] where concentration of DNA is expressed as base pair molarity. (D) A comparison of the fluorescence enhancement on DNA addition shown for all of the isomers.

recognition patterns of these symmetrical derivatives are expected to be different from Hoechst. It is known that for Hoechst 33258 and other asymmetrical "head-to-tail" analogues, the bisbenzimidazolic unit recognizes three base pairs (bp) with each benzimidazole recognizing 1.5 bp (shown in Figure 11).[8] Unlike Hoechst, the "head-to-head" analogues have been shown by Neidle and co-workers to cover 4 bp with each benzimidazole unit recognizing 2 bp.[19]

However, when the binding of these molecules to DNA was examined, it was found that whereas *p*- and *m*-pyben showed strong binding affinity to *ds*-DNA, the interaction of *o*-pyben with DNA was weaker. For all physical studies a 2 mM solution of the compounds was prepared in DMSO, which was then injected in appropriate volumes in aqueous buffer where they formed stable solutions.

All molecules showed absorbance with λ_{max} in the 342−345 nm range in buffer. When excited at the respective λ_{max} of the compound in solution, fluorescence emission was observed depending on the solvent (Figure S1, Supporting Information). The emission behavior of the molecules has been examined in a range of solvents, which included polar solvents such as water (at pH = 7), methanol, and *n*-propanol, aprotic solvent dioxane, and nonpolar toluene. All three isomers showed minimal fluorescence in neutral aqueous medium. The emission intensity increased with decreasing solvent polarity, followed by blue-shifted emission maxima, indicative of an increasing hydrophobic environment. This became apparent when we compared the emission characteristics of the compounds in buffer or other protic solvents such as methanol with that in aprotic solvent such as dioxane or toluene. Additionally it was observed that the inherent fluorescence of the *o*-pyben in all solvents was higher than its isomers (Figure S1). The intrinsically similar emission behavior of all of the compounds argues that the comparatively low fluorescence enhancement of the *o*-pyben on DNA addition, with respect to its *meta* and *para* analogues, arose mainly because of the differences in binding interaction and not because of any inherent differences in its emission characteristics.

Fluorescence Titration. The bisbenzimidazole class of dyes such as Hoechst are nonfluorescent in aqueous solution at neutral pH but on binding to *ds*-DNA show a remarkable enhancement of fluorescence emission, with quantum yield increasing by ∼20- to 30-fold. This fluorescence increase upon binding to *ds*-DNA may be attributed to exclusion of solvent water molecules or to restricted internal mobility of the fluorophore upon binding to double helical DNA.[27] All three isomers of the pyridine derivatized bisbenzimidazoles showed minimal fluorescence in neutral aqueous medium. The increased emission intensity on DNA addition, accompanied by blue-shifted emission maxima, was indicative of an increased hydrophobic

(27) Cosa, G.; Focsaneanu, K. S.; McLean, J. R. N.; McNamee, J. P.; Scaiano, J. C. *Photochem. Photobiol.* **2001**, *73*, 585.

TABLE 1. Apparent Binding Constants (*K*) of Bis-2-(*n*-pyridyl)-1*H*-benzimidazoles for the Three Types of DNA Used[a]

ligand	CT DNA $K \times 10^7$ (M^{-1})	$[Poly(dA\text{-}dT)]_2$ $K \times 10^7$ (M^{-1})	[Poly(dA)-Poly(dT)] $K \times 10^7$ (M^{-1})
p-pyben	10.0	1.3	4.2
m-pyben	9.0	1.9	4.0
o-pyben	2.0	0.6	0.8

[a] Each set of titration experiment was repeated at least twice, and the calculated binding constants were found to be within ±5%.

environment in the DNA groove.[27] The emission intensity in the presence of a saturating concentration of DNA was maximum for the *meta* derivative, followed by the *para* analogue, whereas that for the *ortho* analogue was the least (Figure 1). The difference between *o*-pyben and *p*-pyben was not too high, but emission behavior of the two molecules in a range of solvents (Figure S1) showed that the inherent fluorescence intensity of the free-ligand was lower for *p*-pyben than *o*-pyben. As the intrinsic fluorescence of the free *ortho* derivative in the absence of DNA in buffer was higher than that of its isomer, this suggests that the comparatively low fluorescence enhancement of the *ortho* isomer, on DNA addition, arose mainly as a result of its poor binding interaction.

The observed increase in fluorescence saturated in all cases at a certain base pair to compound ratio characteristic of each compound/duplex type.

Additionally, titration performed with $[Poly(dG\text{-}dC)]_2$ did not cause any fluorescence enhancement of any of the molecules (Figure S2), indicating an A-T selective mode of binding.

The binding constants calculated following the McGhee−von Hippel equation and nonlinear Scatchard plots also indicated a much weaker binding of the *ortho* derivative to DNA compared to the *meta* and *para* analogues. The data are shown in Table 1.

Circular Dichroism. CD spectroscopy provides a powerful tool to detect and characterize the complexes of DNA duplexes with Hoechst 33258 as with other ligands.[28] Neither the duplex DNA nor the ligand alone exhibit CD signals at the wavelengths of absorbance of the ligands. However, the intrinsically achiral ligand molecules acquired an induced circular dichroism (ICD) on binding to DNA. We have used CD to qualitatively compare the interaction of the isomers to *ds*-DNA. The *para* and *meta* derivatives showed a moderate ICD at 350 nm, when titrated into *ds*-DNA (Figure 2B and C). In contrast, the *ortho* derivative showed no ICD under similar conditions (Figure 2A). When plotted against concentration of compounds to nucleotide phosphate, the observed ICD signals increased for *p*- and *m*-pyben and reached saturation characteristic of each ligand's DNA binding property. This proved significant DNA binding by the *meta* and *para* analogues and farther established the weaker DNA binding interactions of the *ortho* derivative.

Thermal Denaturation of DNA. Duplex DNA melting, i.e., thermal helix to coil transition is associated with a hyperchromicity of the 260 nm absorption band, and the melting temperature of DNA sequences [Poly(dA)-Poly(dT)] and $[Poly(dA\text{-}dT)]_2$ in presence of the drugs were determined by following the absorbance at 260 nm (Figure 3A and B). The stabilization of DNA in presence of *p*- and *m*-pyben was clearly evident from the enhancement of DNA melting temperatures, indicating

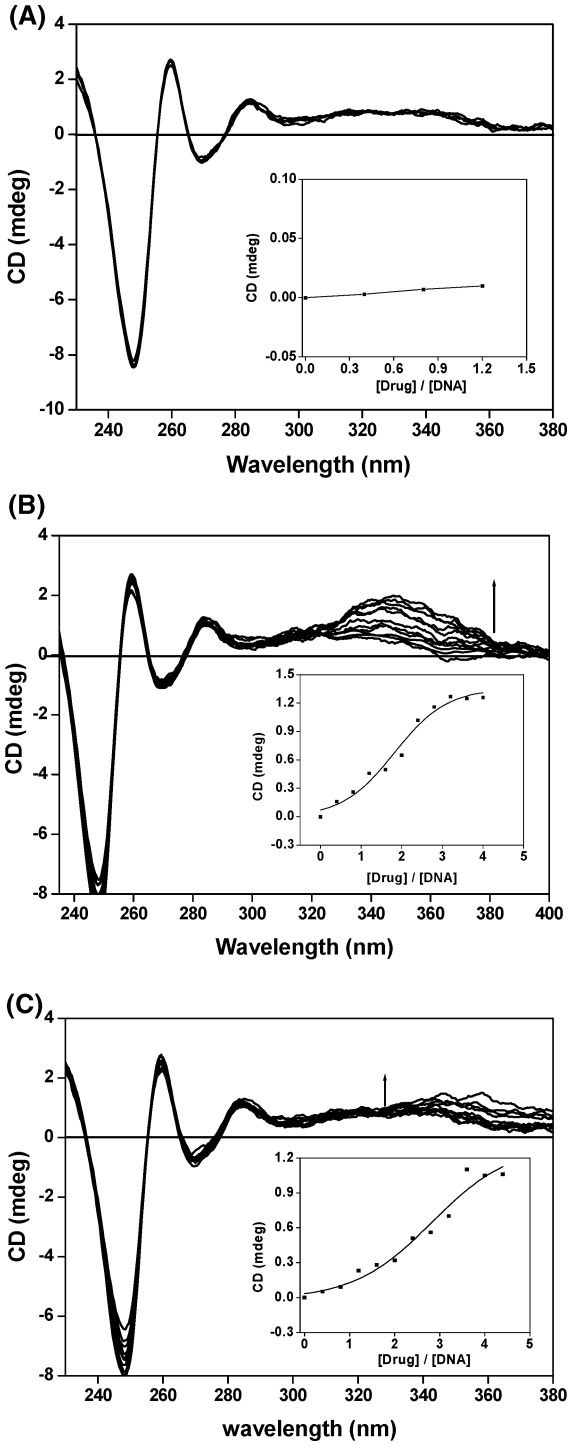

FIGURE 2. Compound titrated into 10 μM of [Poly(dA)-Poly(dT)] in buffer (50 mM Tris-HCl, 100 mM NaCl, 0.1 mM EDTA, pH = 7.4): (A) *o*-pyben, (B) *m*-pyben, and (C) *p*-pyben. Inset: ICD versus [drug]/[DNA].

duplex stabilization comparable to that of parent Hoechst 33258. With *o*-pyben, however, the enhancement was <1 °C, indicating poor duplex stabilization in the presence of this compound.

The melting temperature enhancements have been summarized in Table 2. Taken together the collective data obtained from all of the DNA binding experiments established the fact that whereas *p*- and *m*-pyben had significant interaction with DNA, binding affinity of *o*-pyben to *ds*-DNA was quite weak.

(28) Canzonetta, C.; Caneva, R.; Savino, M.; Scipioni, A.; Catalanotti, B.; Galeone, A. *Biochim. Biophys. Acta* **2002**, *1576*, 136.

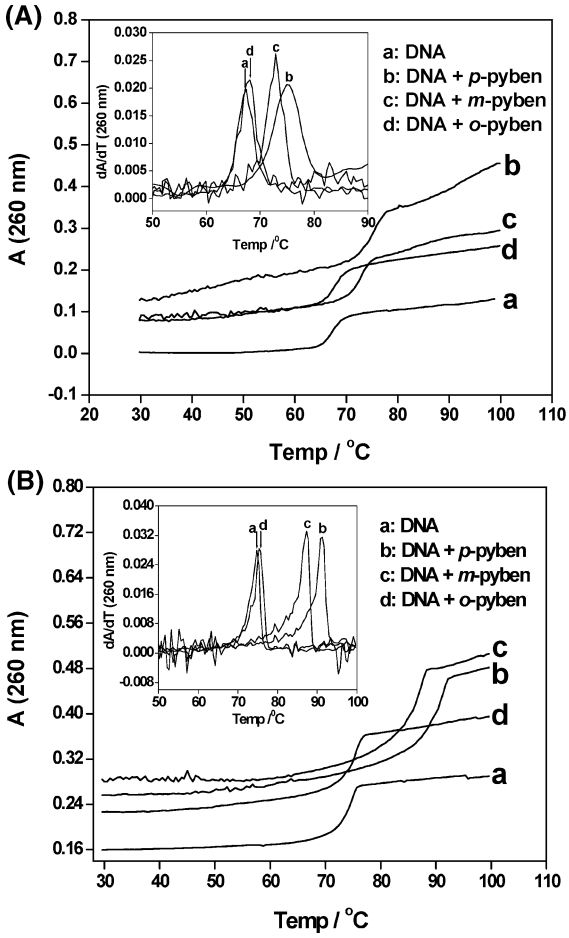

FIGURE 3. Thermal melting profiles at saturating [drug]/[DNA] ratios after incubation for 24 h in 50 mM Tris-HCl, 100 mM NaCl, 0.1 mM EDTA. Plots are shown as the changes in absorbance at 260 nm versus temperature (°C). DNA used: (A) $[Poly(dA\text{-}dT)]_2$, (B) [Poly (dA)-Poly(dT)]. Insets show the first derivative plots of the heating scan.

TABLE 2. Melting Temperature Obtained by Following Absorption at 260 nm

	$[Poly\ (dA\text{-}dT)]_2$		[Poly(dA)-Poly(dT)]	
compound	T_m (°C)	ΔT_m[a] (°C)	T_m (°C)	ΔT_m[a] (°C)
	67.1		74.7	
p-pyben	75.5	8.4	91.1	16.4
m-pyben	73.0	5.9	87.4	12.7
o-pyben	67.5	0.4	75.4	0.7
Hoechst	80.0	12.9	90.4	15.7

[a] ΔT_m values were the differences in melting temperatures between uncomplexed and ligand-bound duplexes and were determined by first derivative analysis. Each melting experiment was repeated twice, and the melting temperature differences obtained from different sets of experiments were within ±0.1 °C. The average of the two data has been reported.

Computational Analysis. The main factors that govern minor groove binding of a drug are the following: (a) isohelicity of the drug with the minor groove of DNA, (b) hydrogen bond donor groups on the ligand and their proper phasing with the nucleobases at the floor of the minor groove, and (c) net positive ligand charge.[29,30] Previous studies, experimental and computational, reported in the literature show that because of the high concentration of H^+ ion near the DNA surface there is a predicted lowering of pH near DNA compared to bulk water.[31,32] Hence the molecule should remain partially protonated on the DNA surface. There might be some variations in the protonation pK_a values of the three molecules owing to the position of the pyridine nitrogen, but the variations should not cause such a drastic difference in their DNA binding affinity. Next, all three molecules, being bisbenzimidazole derivatives like Hoechst, are expected to retain the ability to act as hydrogen bond donors to the DNA bases. Despite the apparent similarity among the three molecules, the DNA binding characteristic of the *o*-pyben varied considerably from that of its *meta* and *para* analogues. In order to rationalize this difference, we ventured to analyze closely the conformations of the molecules.

Gas-Phase Conformations and Effect of Solvation. Each of the three molecules were optimized at the B3LYP/6-31G* level of theory. For this purpose two relevant conformations were considered, one in which the protons attached to the benzimidazole N face the inner concave edge and one where they are on the convex edge, denoted by **1** and **2** respectively. The B3LYP/6-31G* stabilized structures of **1** and **2** for all three molecules in the gas phase are shown in Figure 4. For all of the isomers, conformation **1** was found to be more stable than **2** in the gas phase (Table 3). The energy differences between **1** and **2** are relatively smaller for *m*-pyben and *p*-pyben. However, for *o*-pyben, conformation **1** was found to have energy much lower than that of **2**. Indeed the former was found to be ∼20 kcal/mol more stabilized than the latter (Table 3).

Next we wanted to investigate the effect of solvation on the conformational preference of the isomers and on the relative stability of the conformers. We performed full optimization using the Onsager model taking $\epsilon = 78.4$. The relative energy values are given in Table 3. We observed minor stabilization of conformer **2** with respect to **1** for *p*-pyben and *m*-pyben. However, for *o*-pyben, stabilization of **1** was still much higher compared with **2**, and the energy difference between the two conformers was very similar to that observed in the gas phase (∼20 kcal/mol in both gas and aqueous phases. See Table 3). Next we computed single point energy differences between the conformers **1** and **2** for all three isomers using Polarizable Continuum Model (PCM). For *p*-pyben and *m*-pyben the energy values obtained by using the Onsager model and that obtained from single point energy calculation using PCM were nearly similar. Also, relative energy values showed marginal stabilization of **2** compared to **1**. However, for *o*-pyben the energy difference between the conformers was lowered to ∼10 kcal/mol when PCM was used, but it was observed that conformer **1** was still much more stable compared to **2**. Thus irrespective of the model used, the dramatic stabilization of conformer **1** of *o*-pyben in both gas and aqueous phases was established.

An interesting observation made for the *ortho* derivative was that in **1**, which was established as the more stable conformation, the pyridine nitrogen (N1) and imidazole proton (H3) were intramolecularly hydrogen bonded (2.46 Å) (Figure 5).

Next, an examination of the torsion angles between the pyridine and one benzimidazole ring (α) revealed another important difference (Table 4). Between the tautomers **1** and **2** there existed a significant variation in torsional angle (α) for all of the molecules. However, for *o*-pyben, the results were most dra-

(29) Spink, N.; Brown, D. G.; Skelly, J. V.; Neidle, S. *Nucleic Acids Res.* **1994**, *22*, 1607.
(30) Neidle, S. *Biopolymers* **1997**, *44*, 105.
(31) Lamm, G.; Pack, G. R. *Proc. Natl. Acad. Sci. U.S.A.* **1990**, *87*, 9033.
(32) Lamm, G.; Wong, L.; Pack, G. R. *J. Am. Chem. Soc.* **1996**, *118*, 3325.

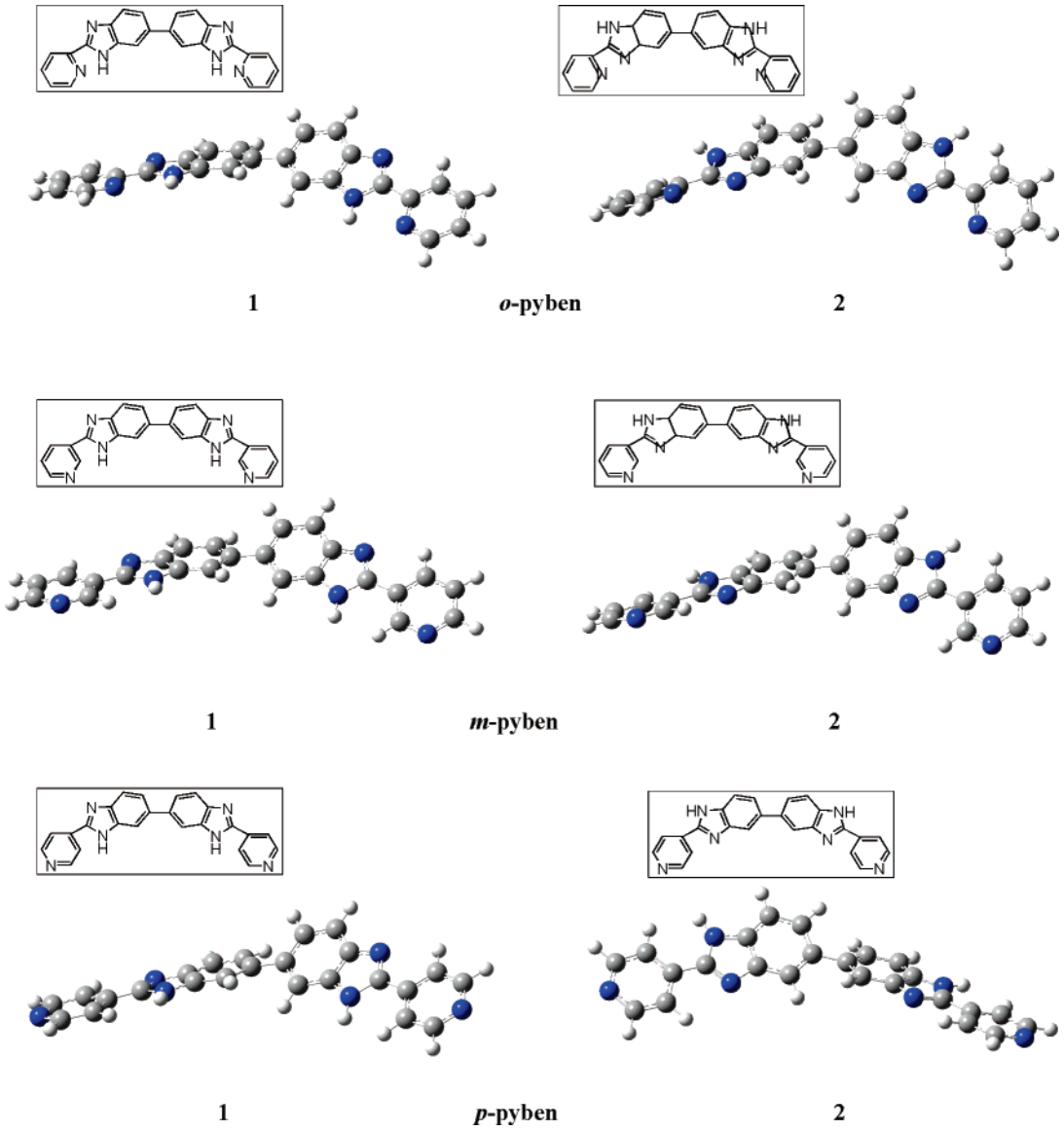

FIGURE 4. Energy minimized structures in the gas phase for the three isomers at the B3LYP/6-31G* level of theory.

TABLE 3. Relative Energies (kcal/mol) for Conformers of *o*-Pyben, *m*-Pyben, and *p*-Pyben in Gas Phase and in Water at the B3LYP/6-31G* Level

compound	1	2
p-pyben (gas)	0.0	0.6
p-pyben (aq)[a]	0.7	0.0
p-pyben (aq)[b]	0.9	0.0
m-pyben (gas)	0.0	2.7
m-pyben (aq)[a]	1.2	0.0
m-pyben (aq)[b]	1.1	0.0
o-pyben (gas)	0.0	20.3
o-pyben (aq)[a]	0.0	19.9
o-pyben (aq)[b]	0.0	9.7

[a] Calculated in water using the Onsager model using dielectric constant $\epsilon = 78.4$. [b] Single point PCM energy differences for conformers **1** and **2** in water.

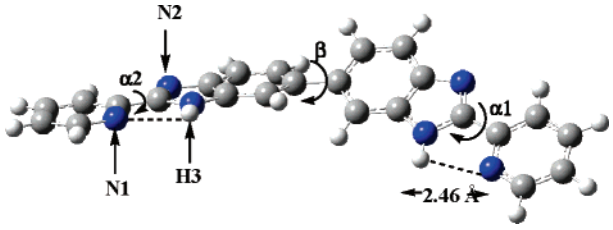

FIGURE 5. Structure of conformer **1** of the *o*-pyben minimized at the B3LYP/6-31G* level. The atom numberings for pyridine nitrogen (N1), benzimidazole nitrogen (N2), and benzimidazole proton (H3), used in the text, are indicated by arrows. α1, α2, and β denote the dihedral angles about the bonds indicated by the arrows. The dotted line indicates an intramolecular hydrogen bond between N1 and H3, distance being 2.46 Å.

matic. Pyridine and benzimidazole rings were coplanar (α = 0.3° gas phase and 0.8° aqueous phase) in **1** but deviated largely from planarity in **2** (α = 22.8° gas phase and 19.5° aqueous phase). The torsional angle (β) between two benzimidazole rings, however, remained largely invariant in all cases (Table 4). As expected, a biphenyl-type twist (twisting angle ~40°)[33] was present between the benzimidazole rings in all three isomers.

Therefore, it appeared that the preference for conformation **1** in *o*-pyben was due to a high degree of planarity between the pyridine and benzimidazole rings. It is possible that the

TABLE 4. Torsion Angles α and *β* in Gas and Aqueous Phases for Conformers 1 and 2 of the Three Bisbenzimidazoles at the B3LYP/6-31G* Level

	1			2		
compound	α1	α2	*β*	α1	α2	*β*
p-pyben (gas)	2.5	2.5	39.4	2.1	2.1	40.4
p-pyben (aq)[a]	1.4	1.4	38.9	3.2	3.2	38.6
m-pyben(gas)	2.2	2.2	39.4	7.9	7.9	40.2
m-pyben (aq)[a]	6.4	6.3	39.5	11.8	11.8	36.5
o-pyben (gas)	0.3	0.3	39.6	22.8	22.8	40.3
o-pyben (aq)[a]	0.8	0.8	38.9	19.5	19.5	38.0

[a] Calculated in water using the Onsager model using dielectric constant $\epsilon = 78.4$.

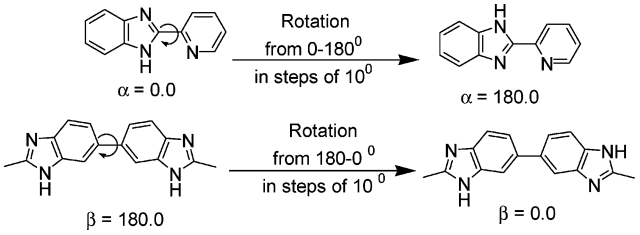

FIGURE 6. Compound broken into fragments for potential energy surface scan. The arrows indicate the bonds about which rotations were performed.

intramolecular hydrogen bonding existing in *o*-pyben led to coplanarity between the rings and consequently the cooperative effects of hydrogen bonding and conjugation caused such high stabilization of **1** compared to that of **2**. It is known for bisbenzimidazolic drugs that these hydrogens (H3) attached to the benzimidazole N face the DNA minor groove floor and play crucially important roles in forming bifurcated hydrogen bonds to the N3 of adenine and O2 of thymine.[29,30,34]

It is also known that for high affinity binding, proper phasing of the ligand subunits with the edges of the DNA base pairs in the minor groove is an important criterion, and this often requires the ligand to be twisted about the bonds connecting the individual subunits.[12,34] To examine the importance of rotation about the (C−C) bonds connecting the rings, the molecule was broken into two fragments, pyridine-benzimidazole and benzimidazole-benzimidazole. The torsion angle about the bond connecting the former units is denoted by α and the latter by *β* (Figure 6), and a potential energy surface was scanned by systematically varying α and *β* in steps of 10°.

Pyridine-benzimidazole. The symmetrical and near-symmetrical rotational profiles for the torsional angle α obtained for the *para* and *meta* isomers in the gas and aqueous phases account for the very small energy difference between **1** and **2** (Figure 7A and B). When the minimum energy conformations (corresponding to $\alpha \approx 0°$) of all of the isomers were compared, the calculated results showed that the *ortho* derivative was lower in energy by ∼ 6.0 kcal/mol compared to *m*-pyben and *p*-pyben in the gas phase. In the aqueous phase the difference of energy was lowered (∼3.0 kcal/mol) compared to the gas phase. For *o*-pyben, a second local minimum was obtained at $\alpha \approx 160°$, which however was much stabilized in the aqueous phase compared to the gas phase. The energy difference between the troughs ($\alpha \approx 0°$ and $\alpha \approx 160°$) was reduced from 10.4 kcal/mol in the gas phase to 4.0 kcal/mol in the aqueous phase. This was in keeping with the previous results obtained from single point energy calculation using PCM, which showed that the energy difference between the conformers **1** and **2** was reduced on solvation. The α values ($\alpha \approx 0°$ and $\alpha \approx 160°$) for *o*-pyben, at the two minima in the energy profiles in Figure 7A and B, also corresponded well with the torsion angle values (α) of conformers **1** and **2** respectively in the full-optimized structures (Table 4).

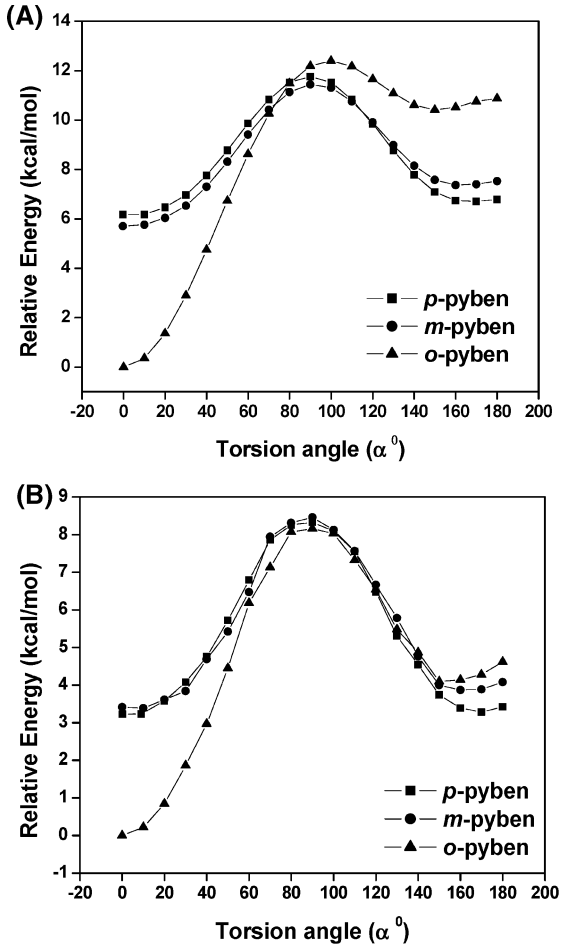

FIGURE 7. Evolution of the gas-phase (A) and aqueous-phase (B) conformational energy of the pyridine-benzimidazole fragment as a function of the torsional angle α computed at the B3LYP/6-31G* level. Aqueous-phase calculation was done using PCM taking water as solvent at the B3LYP/6-31G* level.

For complete ring flipping, all three isomers had to cross an energy barrier corresponding to $\alpha = 90°$. The calculated rotational barriers for *m*- and *p*-pyben were ∼6.0 kcal/mol (gas phase) and ∼5.0 kcal/mol (aqueous phase), whereas it was ∼12.0 kcal/mol, almost doubled, for *o*-pyben (Figure 7A). However, in the aqueous phase, this value was reduced to 8.0 kcal/mol for *o*-pyben (Figure 7B). (See Supporting Information Tables S32 and S33 for tabulated relative energy values for all of the isomers at the B3LYP/6-31G* and RHF/6-31G* levels of calculation).

It is known that the Hoechst molecule is forced to adopt a twisted conformation to allow the benzimidazole hydrogen bond donors to remain in phase with the base acceptor sites and for the ligand to follow the groove topology. The close fit between

(33) Grein, F. *J. Phys. Chem. A* **2002**, *106*, 3823.
(34) Clark, G. R.; Squire, C. J.; Gray, E. J.; Leupin, W.; Neidle, S. *Nucleic Acid Res.* **1996**, *24*, 4882.

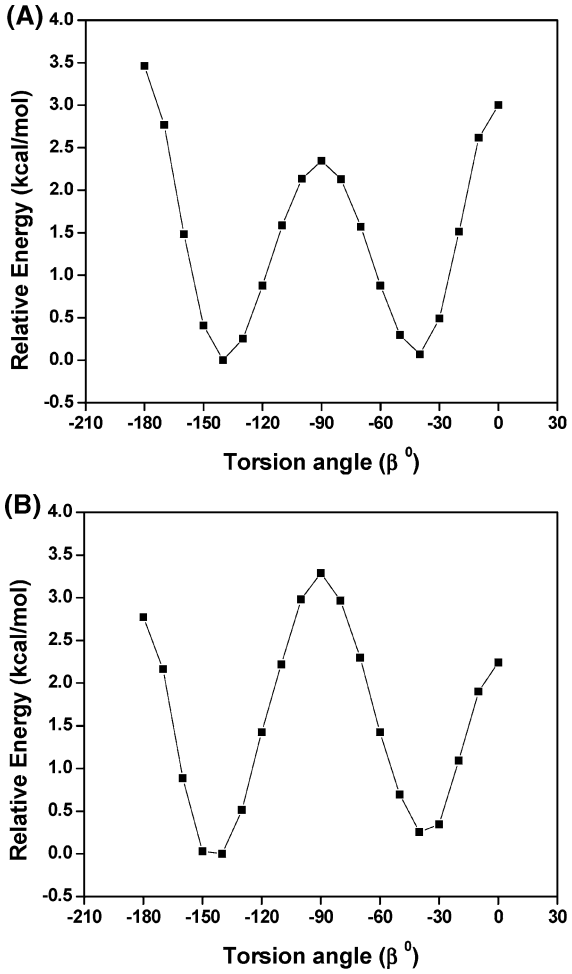

FIGURE 8. Evolution of the gas-phase (A) and aqueous-phase (B) conformational energy of the benzimidazole-benzimidazole fragment as a function of the torsional angle β computed at the B3LYP/6-31G* level. Aqueous-phase calculation was done using PCM taking water as solvent at the B3LYP/6-31G* level.

TABLE 5. Calculated Mulliken Charge Density on the Pyridine N (N1) and Benzimidazole N (N2) in the Conformers 1 and 2 of the Three Compounds at the B3LYP/6-31G* level[a]

	1		2	
compound	N1	N2	N1	N2
p-pyben	−0.403	−0.570	−0.412	−0.575
m-pyben	−0.412	−0.575	−0.428	−0.582
o-pyben	−0.523	−0.585	−0.445	−0.539

[a] Calculated in water using dielectric constant $\epsilon = 78.4$

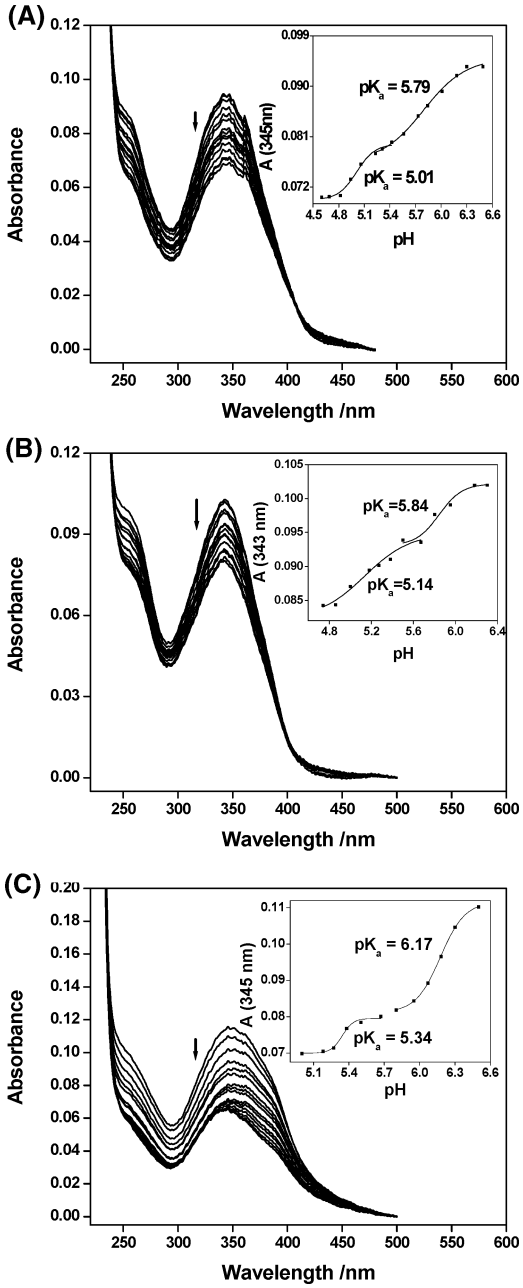

FIGURE 9. (A) *p*-pyben (A), (B) *m*-pyben (B), and (C) *o*-pyben (C) were dissolved at 6 μM in CH_3COONa/HCl buffer (pH = 6.8), and HCl was incrementally added in 1−2 μL volumes. Arrows indicate change in absorbance on acidification. Inset: the absorbance was plotted versus the pH values and the curves were fitted into the sigmoidal function. The midpoint of the sigmoidal curve on the *x*-axis was taken as the pK_a value.

the ligand and the minor groove is maintained by rotations about the bonds connecting the individual rings.[12] Hence for optimum binding of any drug to the DNA grooves the former should have sufficient conformational flexibility to adapt to the curvature of the groove.[34] For a structurally related symmetrical bisbenzimidazole derivative, the crystal structure of the DNA bound drug is known (PDB code 1FTD).[20] The torsional angle (between the phenyl and benzimidazole rings) corresponding to α was found to be close to 19°. From Figure 7A and B, it was obvious that for any deviation from planarity, the energy gradient for *o*-pyben was much steeper than *m*- or *p*-pyben. Hence the restricted rotational mobility about the bond connecting the pyridine and benzimidazole rings gives a conformational rigidity to *o*-pyben. This makes any out of plane rotation about the said bond energetically disfavored, which might contribute toward the poor binding affinity of *o*-pyben to *ds*-DNA.

Benzimidazole-benzimidazole. Rotation about the bond connecting the two benzimidazole rings generated an energy profile that gave minima around a dihedral angle of ∼40 ° (Figure 8A and B). This finding agrees well with the results obtained from the full optimization calculations, and these values were similar for all three isomers. For the biphenyl twist, barriers heights of 3.5 kcal/mol at $\beta = 0°$ and 2.4 kcal/mol at $\beta = 90°$

TABLE 6. Experimental pK_a Values for the Three Benzimidazole Derivatives in Water[a]

compound	pK_{a1}	pK_{a2}	pK_{a3}	pK_{a4}
p-pyben	5.8 ± 0.03	5.0 ± 0.02	4.1 ± 0.05	3.1 ± 0.03
m-pyben	5.8 ± 0.04	5.1 ± 0.03	4.1 ± 0.02	3.1 ± 0.03
o-pyben	6.2 ± 0.01	5.3 ± 0.02	3.8 ± 0.02	2.6 ± 0.02

[a] The results are the average of two independent sets of experiments.

were found in the gas phase. Hence, the feature distinguishing *o*-pyben from its other isomers was the conformational preference of the pyridine-benzimidazole fragment.

pK_a Determination. We rationalized that if indeed intramolecular hydrogen bonding existed between the pyridine N1 and benzimidazole H3 in *o*-pyben, then it should be reflected in the protonation characteristic of the pyridine nitrogen (N1). To secure a better understanding of the bis-2-(*n*-pyridyl)-1*H*-benzimidazoles ($n = 2, 3, 4$), protonation characteristics of each compound in aqueous media were ascertained by experimental pK_a determination. The molecules have four protonation sites each, namely, the two benzimidazole N2 and the two pyridine N1. The calculated Mulliken charges for these molecules qualitatively suggested that benzimidazole nitrogens (N2) would be the first protonation sites compared to pyridine nitrogens (N1) (Table 5), and the conformer **1** of *o*-pyben would have a proton affinity higher than that of *p*-pyben and *m*-pyben. To quantify the proton affinities of the benzimidazole nitrogens (N2) of *o*-, *m*-, or *p*-pyben, free energy of protonations were calculated at the B3LYP/6-31G* level of theory. The computed free energy of N2 protonation (−239.4 kcal/mol) for **1** of *o*-pyben was found to be higher than that of *m*- and *p*-pyben (−234.5 and −232.1 kcal/mol, respectively).

Protonations from pH 6.8−4.5 and from pH 4.5−2.2 were performed using different buffer systems (see Experimental Section). The higher pH range from 6.5 to 4.8 expectedly covered the protonation equilibria of the two benzimidazole nitrogens. Protonation was accompanied by hypochromicity of the ∼350 nm absorption band for all three compounds (Figure 9) and also by a marked blue shift for *o*-pyben, which became more pronounced at pH < 4.5. The pK_{a1} and pK_{a2} of *p*-pyben and *m*-pyben were almost similar in value, being ∼5.8 and ∼5.1, respectively. However, for *o*-pyben the pK_a values for the benzimidazole nitrogens (N2) were higher, around 6.2 and 5.3 (Table 6).

Next, if the pyridine N (N1) in *o*-pyben is indeed involved in intramolecular hydrogen bonding with the benzimidazole H (H3), as deduced from the computational analyses, then it should have a lower pK_a, because protonation of N1 might lead to steric crowding with benzimidazole H3, which would resist such

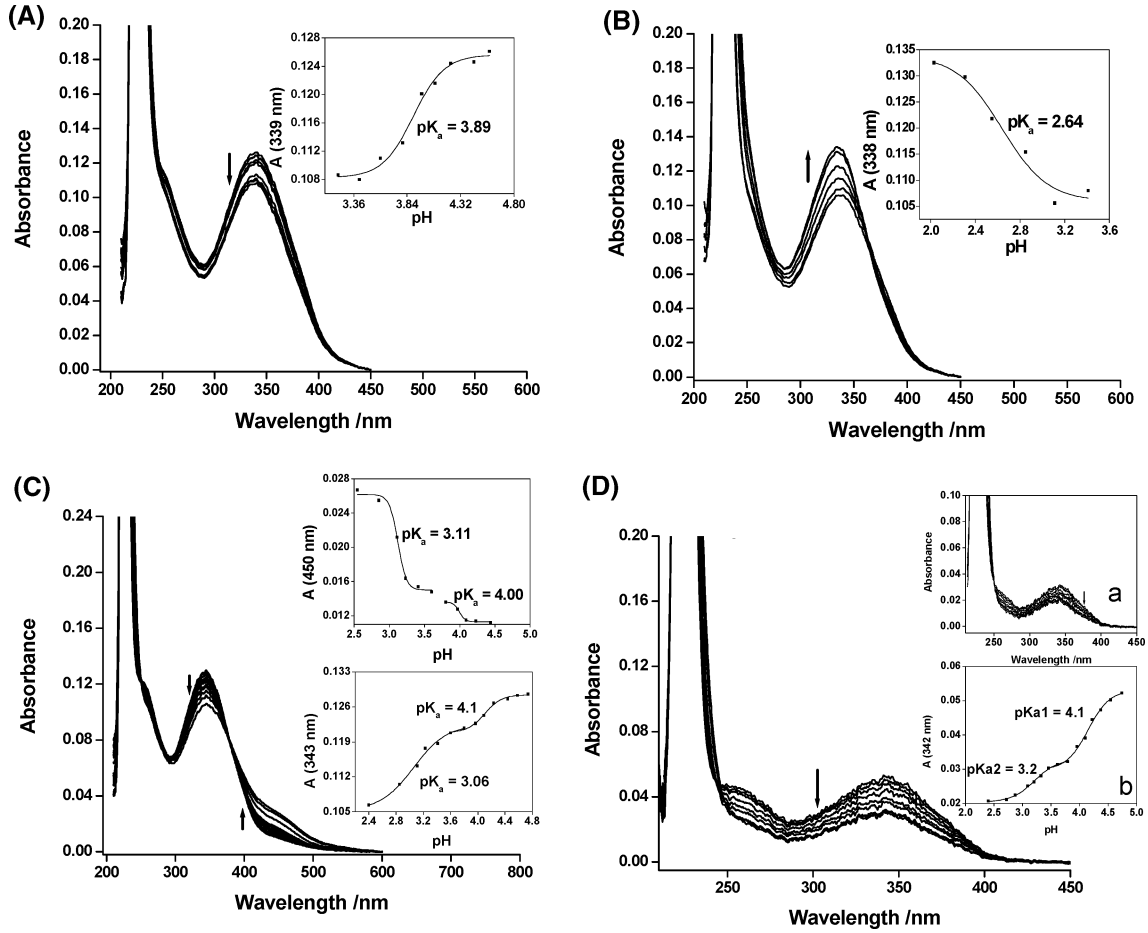

FIGURE 10. Acid−base titration followed by absorption. Each of the compounds (6 μM) was dissolved in HCOONa/HCl buffer (pH = 4.7), and HCl was added in 1−2 μL volumes. (A) *o*-Pyben (pH = 4.5−3.3), (B) *o*-pyben (pH = 3.3−2.2). Insets: the absorbance for *o*-pyben at 338 nm versus pH. (C) *p*-Pyben (pH = 4.7−2.3). Inset: absorbance at 345 and 450 nm plotted versus the pH. (D) *m*-Pyben (pH = 4.7−3.5). Inset a: absorbance at pH = 3.5−2.4. Inset b: absorbance at 342 nm versus pH. Arrows indicate change in absorbance on acidification. The absorbance versus pH curves were fitted into a sigmoidal function. The midpoint of the sigmoidal curve on the *x*-axis was taken as the pK_a value.

protonation. This again was the observed result. The protonation pK_a of the two pyridine nitrogens (pK_{a3} and pK_{a4}, Table 6) were indeed much lower in *o*-pyben compared with those of *p*-pyben or *m*-pyben. In the case of *p*-pyben and *m*-pyben (Figure 10C and D), the long wavelength absorption did not shift much from the 345 nm value in the entire pH range of 6.5−2.5. Acidification was accompanied by only a hypochromicity of the 345 nm band, and below pH 4.5 a shoulder appeared for *p*-pyben at 450 nm, which increased in intensity with further acidification (Figure 10C). For *o*-pyben, however, acidification below pH 4.5 caused the long wavelength band to be blue-shifted from 345 to 338 nm and finally to 334 nm at pH 2.5 (Figure 10A and B). Moreover further acidification below pH 3.5 caused hyperchromicity of the long wavelength band (Figure 10B). The pH range between 4.5 and 2.5 is associated with pyridine protonation, and protonation of pyridine N1 would lead to steric crowding with the benzimidazole H3. Steric crowding may lead to non-coplanarity between the pyridine and benzimidazole rings; blue-shifting and hyperchromicity of the absorption maxima on acidification probably was indicative of loss of planarity (Figure 10A and B). The experimentally obtained pK_a values are summarized in Table 6. Such noticeable differences in absorption on protonation of *o*-pyben, compared to its isomers, draws attention toward inherent structural features distinguishing the former. We inferred that these differences probably arose owing to the intramolecular hydrogen bonding existing in *o*-pyben.

Conclusions

The combined experimental data established weaker DNA binding affinity of the *ortho* isomer compared with that of its *para* and *meta* analogues. To rationalize this result we have probed closely into the inherent conformational preferences of all three isomers.

Earlier reports have shown that the nonpolar dielectric environment experienced by Hoechst in the minor groove of alternating Poly[AT] DNA ($\epsilon \approx 20$) is much closer to the dielectric environment of the gas phase ($\epsilon \approx 1$) than to that of water ($\epsilon \approx 80$).[35] Hence it can be assumed that the conformational preference in the gas phase will be closer to the conformation adopted by the molecules when bound to the DNA minor groove. The computational and experimental results taken together indicate that the *ortho* derivative exists as conformation **1** in both aqueous and gaseous environments, and the preferential stability of the conformation **1** with respect to that of **2** was surprisingly high for this isomer. We found that the presence of intramolecular hydrogen bonding in **1** confers this stability and high conformational rigidity to *o*-pyben about the bond connecting the pyridine and benzimidazole rings. Experimental pK_a determination indirectly substantiated the presence of intramolecular hydrogen bonding in *o*-pyben. The reduced binding affinity of the *ortho* isomer to *B*-DNA can be accounted for in two ways. First, it is known that twist and flexibility in the drug structure are essential criteria for DNA binding. The four linked groups in Hoechst 33258 can have dihedral angles of up to 15−20° between them.[30] Conformational rigidity of *o*-pyben probably restricts it from acquiring optimum shape complimentarity with the minor groove required to maximize van der Waals attraction, whereas *m*- and *p*-pyben can attain

(35) Jin, R.; Breslauer, K. J. *Proc. Natl. Acad. Sci. U.S.A.* **1988**, *85*, 8939.

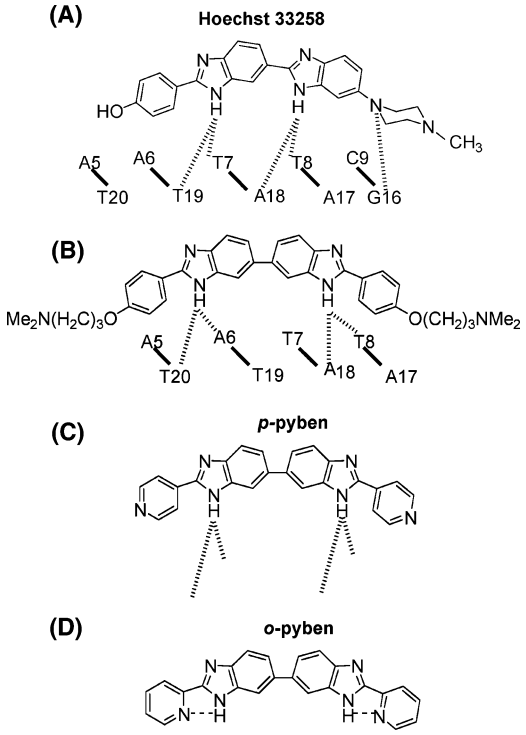

FIGURE 11. Schematic representation of bifurcated hydrogen bonding between the benzimidazolic protons in (A) Hoechst 33258 and DNA bases adenine A and thymine T, shown by dashed lines (PDB code 8BNA),[8] (B) 2,2-bis[4′-(3′-dimethylamino-1″-propyloxy)phenyl]-5,5-bi-1*H*-benzimidazole (PDB code 1FTD),[20] (C) *p*-pyben with benzimidazole protons hydrogen bonding with DNA bases, in a manner similar to a structurally allied system shown in panel B, and (D) *o*-pyben with the crucial benzimidazole protons involved in intramolecular hydrogen bonding.

the conformation to bind with *ds*-DNA favorably at lower energy costs. Next, in parent Hoechst 33258, the benzimidazole hydrogens are known to form bifurcated hydrogen bonds with the N3 of adenine and O2 of thymine bases in the DNA minor groove. On the basis of the energy minimized conformations of the three isomers, it is clear that the pyridine N in the *ortho* derivative is within the hydrogen-bonding distance of the benzimidazole proton. Hence such intramolecular hydrogen bonding makes the crucial benzimidazole protons less available for hydrogen bonding with DNA bases (Figure 11); however, this is not the case with the corresponding *meta* and *para* isomers. This is reflected in the high binding affinity of these two molecules to *ds*-DNA. The present study thus describes how minor chemical alterations in a set of isomeric bis-2-(*n*-pyridyl)-1*H*-benzimidazoles alter their molecular structure and geometry, which in turn significantly influences their DNA binding affinity on the floor of the minor groove.

Experimental Section

Synthesis. All starting materials were procured from best known commercial sources and used without farther purification. The compounds were synthesized by one step oxidative condensation between 3,3′-diaminobenzidine and 2-, 3-, or 4′-pyridine carboxaldehyde in dry nitrobenzene at 120 °C following procedures described in literature.[20]

DNA Binding. DNA binding experiments were performed using calf thymus (CT DNA), [Poly(dA)-Poly(dT)], [Poly(dA-dT)]$_2$, and [Poly(dG-dC)]$_2$. These were obtained from best known commercial

sources and used as received. Concentrations of the nucleic acids were determined spectrophotometrically and expressed as base pairs with ϵ values (M^{-1} cm^{-1}) as indicated: calf thymus (CT) DNA, $\epsilon_{258} = 13600$; [Poly(dA-dT)]$_2$, $\epsilon_{262} = 13200$; [Poly(dA)-Poly(dT)], $\epsilon_{262} = 12000$; [Poly(dG-dC)]$_2$, $\epsilon_{262} = 16800$.[7] For the DNA binding experiments, a stock solution of the compounds of concentrations in the range of ~2 mM were prepared in dimethyl sulfoxide (DMSO) and stored at −4 °C. Buffers used for all of the studies were 50 mM Tris-HCl, 100 mM NaCl, and 0.1 mM EDTA (pH 7.4).

Fluorescence Titration. Fluorescence spectra were recorded on a spectrofluorimeter, with excitation and emission slit width each fixed at 10 nm. A constant ligand concentration (~ 2.0 μM) was titrated with increasing concentration of *ds*-DNA. An interval of 5 min was given between each addition to allow for equilibration. The excitation wavelengths were between 340 and 350 nm for all of the compounds, and the emission maxima were centered at ~440 nm. Different DNA samples, e.g., CT DNA, [Poly(dA-dT)]$_2$, [Poly-(dA)-Poly(dT)], and [Poly(dG-dC)]$_2$, were used for separate titrations. All fluorescence titrations were performed at 25 °C. Binding constants were determined from the fluorescence data. For the repetitive sequences such as [Poly(dA-dT)]$_2$ and [Poly(dA)-Poly-(dT)], where the potential binding sites overlap, the excluded binding-site model (McGhee−von Hippel) applies.[36] The apparent binding constant (K) was determined using the McGhee−von Hippel equation:

$$\frac{r}{C_f} = K(1 - nr)\left(\frac{1 - nr}{1 - (n-1)r}\right)^{n-1} \quad (1)$$

where r = average number of ligands bound per lattice, C_f = concentration of free ligand, n = binding site size, and K = association constant. The nonlinear Scatchard plot obtained in the case of CT DNA was interpreted considering the special case of two independent binding sites.[37] The higher of the two association constants so obtained was attributed to specific binding of the drug molecule in the AT-rich stretches of the DNA minor groove.

Circular Dichroism Measurements. CD spectra were recorded on a spectropolarimeter. CD titrations were carried out by adding progressively increasing amounts of the respective ligands to the cuvette, keeping the DNA concentration (10 μM) constant. An interval of 10 min between each ligand addition was given to allow for equilibration. Although these compounds were achiral, they acquired an induced CD (ICD) on complexing with chiral polynucleotides.[38] The spectra were recorded at a scan rate of 50 or 100 nm/min, and the ICD of the ligands was monitored in the 340−350 nm range.

DNA Melting Temperature (T_m) Measurements. Thermal melting (T_m) measurements were conducted using a spectrophotometer. Cuvettes for the experiments were mounted by a thermistor with the reference cuvette. Temperatures were maintained under computer control and were increased at 0.5 °C/min. The experiments were conducted in 1-cm path length quartz cuvettes stoppered with Teflon caps, in 50 mM Tris-HCl, 0.1 mM EDTA, and 100 mM NaCl buffer. The melting was followed by recording absorbance changes at 260 nm as a function of temperature. The concentration of DNA used was 10 μM for [Poly(dA)-Poly(dT)] and [Poly(dA-dT)]$_2$, determined by measuring the absorbance at 260 nm. The [drug]/[DNA] ratio corresponded to the saturation ratio obtained from fluorescence titration and corresponded to approximately one drug molecule per four base pairs. Prior to the measurement, the DNA was incubated with the respective drug molecules for 24 h. DNA with no drug was used as control. Melting temperatures were determined from first derivative plots.

Computational Methods. All ab initio and DFT (B3LYP)[39] calculations were performed using the Gaussian 98 suite program.[40] Initially, the stable conformers of all of the isomers were optimized at RHF/6-31G* level.[41] For all systems studied, vibrational frequency calculations were carried out to confirm that they converged to true minima. The RHF optimized geometries were taken for B3LYP calculations using the 6-31G* basis set. For each molecule, two tautomeric structures were calculated that were considered most relevant for DNA binding.

For calculations in the aqueous phase, Onsager's reaction field model was employed,[42] where the solute is assumed to occupy a spherical cavity of radius a_0 in the medium. A dielectric constant (ϵ) of 78.39 (water) was used. The permanent dipole of the solute will induce a dipole (reaction field) in the surrounding medium, which in turn will interact with the molecular dipole to lead to stabilization. The volume obtained (see Supporting Information) from gas-phase volume calculations at the B3LYP/6-31G* level was used for the solvation calculation. Single point energy calculation was performed on the stable conformers **1** and **2** using the polarizable continuum model (PCM).[43−45] Natural charges on the benzimidazole and pyridine nitrogens were determined by NBO[46] calculations (Table S23), but as the obtained trends for all three isomers accorded well with the Mulliken charge density, we have reported the latter. We computed the free energy of imidazole protonation from the energy differences between the neutral species and the monoprotonated one in the gas phase.

Next, rotational profiles about the torsional angles between the pyridine-benzimidazole and benzimidazole-benzimidazole units were computed spanning the angles in the range of 0−180° in steps of 10°. The bisbenzimidazole derivatives were broken into fragments as shown in Figure 6. The potential energy scan was done at the B3LYP/6-31G* and RHF/6-31G* levels in the gas phase. The calculations were repeated in water dielectric using the Self-Consistent Reaction Field (SCRF) method with the PCM.[43−45] (The rotational profile generated by RHF/6-31G* level calculations are shown in Figure S3)

Determination of pK_a. Acid−base titrations with ligand solutions in appropriate buffers were carried out with a pH meter. The pH range of 2−7 covered the protonation equilibria of the pyridine and benzimidazole nitrogens. Two sets of experiments were performed covering the pH ranges 4.5−6.8 (AcONa/HCl) and 2.3−

(36) McGhee, J. D.; von Hippel, P. H. *J. Mol. Biol.* **1974**, *86*, 469.
(37) Bloomfield, V. A.; Crothers, D. M.; Tinoco, I., Jr. *Nucleic Acids: Structures, Properties, and Functions;* University Science Books: Sausalito, CA, 2000.
(38) Berova, N.; Nakanishi, K.; Woody, R. W. *Circular Dichroism: Principles and Applications*, 2nd ed.; John Wiley and Sons Inc.: New York, 2000.
(39) (a) Becke, A. D. *J. Chem. Phys.* **1993**, *98*, 1372. (b) Becke, A. D. *J. Chem. Phys.* **1993**, *98*, 5648. (c) Lee, C.; Yang, W.; Parr, R. G. *Phys. Rev. B* **1988**, *37*, 785. (d) Becke, A. D. *Phys. Rev. A* **1988**, *38*, 3098. (e) Slater, J. C. *Quantum Theory of Molecules and Solids*; McGraw-Hill: New York, 1974; Vol. 4.
(40) Frisch, M. J.; Trucks, G. W.; Schlegel, H. B.; Scuseria, G. E.; Robb, M. A.; Cheeseman, J. R.; Zakrzewski, V. G.; Montgomery, J. A., Jr.; Stratmann, R. E.; Burant, J. C.; Dapprich, S.; Millam, J. M.; Daniels, A. D.; Kudin, K. N.; Strain, M. C.; Farkas, O.; Tomasi, J.; Barone, V.; Cossi, M.; Cammi, R.; Mennucci, B.; Pomelli, C.; Adamo, C.; Clifford, S.; Ochterski, J.; Petersson, G. A.; Ayala, P. Y.; Cui, Q.; Morokuma, K.; Malick, D. K.; Rabuck, A. D.; Raghavachari, K.; Foresman, J. B.; Cioslowski, J.; Ortiz, J. V.; Stefanov, B. B.; Liu, G.; Liashenko, A.; Piskorz, P.; Komaromi, I.; Gomperts, R.; Martin, R. L.; Fox, D. J.; Keith, T.; Al-Laham, M. A.; Peng, C. Y.; Nanayakkara, A.; Gonzalez, C.; Challacombe, M.; Gill, P. M. W.; Johnson, B. G.; Chen, W.; Wong, M. W.; Andres, J. L.; Head-Gordon, M.; Replogle, E. S.; Pople, J. A. *Gaussian 98*, Revision A.11.3; Gaussian, Inc.: Pittsburgh, PA, 1998.
(41) Hehre, W. J.; Radom, L.; Schleyer, P. v. R. *Ab Initio Molecular Orbital Theory*; J. Wiley & Sons: New York, 1986.
(42) Onsager, L. *J. Am. Chem. Soc.* **1936**, *58*, 1486.
(43) Miertus, S.; Scrocco, E.; Tomasi, J. *Chem. Phys.* **1981**, *55*, 117.
(44) (a) Praveen Kumar, V.; Ganguly, B.; Bhattacharya, S. *J. Org. Chem.* **2004**, *69*, 8634. (b) Barone, V.; Cossi, M.; Tomasi, J. *J. Comp. Chem.* **1998**, *19*, 404.
(45) Tomasi, J.; Persico, M. *Chem. Rev.* **1994**, *94*, 2027.
(46) Reed, A. E.; Weinstock, R. B.; Weinhold, F. *J. Chem. Phys.* **1985**, *83*, 735.

4.5 (HCOONa/HCl). The compounds were dissolved in buffers of pH 6.8 (AcONa/HCl) and pH 4.5 (HCOONa/HCl), respectively.[25] HCl of appropriate concentration was carefully added in volumes of 1−2 μL, ensuring a pH change of 0.2−0.3 after each addition. The final volume of added HCl did not exceed 2% of the total volume. The absorption spectral changes associated with the protonations of the pyridine and benzimidazole nitrogens were used for pK_a determination.

Acknowledgment. This work was supported by the Department of Biotechnology. We thank the Supercomputer Education and Research Centre (SERC) for computational facilities.

Supporting Information Available: Fluorescence emission of the compounds in different solvents, fluorescence titration with $[Poly(dG\text{-}dC)]_2$, Cartesian coordinates of full-optimized geometry in the gas phase at the RHF/6-31G* level and in the gas and aqueous phases at the B3LYP/6-31G* level, Cartesian coordinates of the monoprotonated species in the gas phase at the B3LYP/6-31G* level, natural charges calculated using NBO analysis, rotational profiles generated by the RHF/6-31G* level of calculation, summary of the potential surface scan, and relative energy values obtained on incremental changes of α and β. This material is available free of charge via the Internet at http://pubs.acs.org.

JO0619433